Scaling Properties of Hyperon Production in Au+Au Collisions at $\sqrt{s_{NN}} = 200$ GeV

J. Adams,[2] M.M. Aggarwal,[29] Z. Ahammed,[44] J. Amonett,[19] B.D. Anderson,[19] M. Anderson,[6] D. Arkhipkin,[12] G.S. Averichev,[11] Y. Bai,[27] J. Balewski,[16] O. Barannikova,[2] L.S. Barnby,[2] J. Baudot,[17] S. Bekele,[28] V.V. Belaga,[11] A. Bellingeri-Laurikainen,[39] R. Bellwied,[47] B.I. Bezverkhny,[49] S. Bhardwaj,[34] A. Bhasin,[18] A.K. Bhati,[29] H. Bichsel,[46] J. Bielcik,[49] J. Bielcikova,[49] L.C. Bland,[3] C.O. Blyth,[2] S-L. Blyth,[21] B.E. Bonner,[35] M. Botje,[27] J. Bouchet,[39] A.V. Brandin,[25] A. Bravar,[3] M. Bystersky,[10] R.V. Cadman,[1] X.Z. Cai,[38] H. Caines,[49] M. Calderón de la Barca Sánchez,[6] J. Castillo,[27] O. Catu,[49] D. Cebra,[6] Z. Chajecki,[28] P. Chaloupka,[10] S. Chattopadhyay,[44] H.F. Chen,[37] J.H. Chen,[38] Y. Chen,[7] J. Cheng,[42] M. Cherney,[9] A. Chikanian,[49] H.A. Choi,[33] W. Christie,[3] J.P. Coffin,[17] T.M. Cormier,[47] M.R. Cosentino,[36] J.G. Cramer,[46] H.J. Crawford,[5] D. Das,[44] S. Das,[44] M. Daugherity,[41] M.M. de Moura,[36] T.G. Dedovich,[11] M. DePhillips,[3] A.A. Derevschikov,[31] L. Didenko,[3] T. Dietel,[13] P. Djawotho,[16] S.M. Dogra,[18] W.J. Dong,[7] X. Dong,[37] J.E. Draper,[6] F. Du,[49] V.B. Dunin,[11] J.C. Dunlop,[3] M.R. Dutta Mazumdar,[44] V. Eckardt,[23] W.R. Edwards,[21] L.G. Efimov,[11] V. Emelianov,[25] J. Engelage,[5] G. Eppley,[35] B. Erazmus,[39] M. Estienne,[17] P. Fachini,[3] R. Fatemi,[22] J. Fedorisin,[11] K. Filimonov,[21] P. Filip,[12] E. Finch,[49] V. Fine,[3] Y. Fisyak,[3] J. Fu,[48] C.A. Gagliardi,[40] L. Gaillard,[2] J. Gans,[49] M.S. Ganti,[44] V. Ghazikhanian,[7] P. Ghosh,[44] J.E. Gonzalez,[7] Y.G. Gorbunov,[9] H. Gos,[45] O. Grebenyuk,[27] D. Grosnick,[43] S.M. Guertin,[7] K.S.F.F. Guimaraes,[36] Y. Guo,[47] N. Gupta,[18] T.D. Gutierrez,[6] B. Haag,[6] T.J. Hallman,[3] A. Hamed,[47] J.W. Harris,[49] W. He,[16] M. Heinz,[49] T.W. Henry,[40] S. Hepplemann,[30] B. Hippolyte,[17] A. Hirsch,[32] E. Hjort,[21] G.W. Hoffmann,[41] M.J. Horner,[21] H.Z. Huang,[7] S.L. Huang,[37] E.W. Hughes,[4] T.J. Humanic,[28] G. Igo,[7] P. Jacobs,[21] W.W. Jacobs,[16] P. Jakl,[10] F. Jia,[20] H. Jiang,[7] P.G. Jones,[2] E.G. Judd,[5] S. Kabana,[39] K. Kang,[42] J. Kapitan,[10] M. Kaplan,[8] D. Keane,[19] A. Kechechyan,[11] V.Yu. Khodyrev,[31] B.C. Kim,[33] J. Kiryluk,[22] A. Kisiel,[45] E.M. Kislov,[11] S.R. Klein,[21] D.D. Koetke,[43] T. Kollegger,[13] M. Kopytine,[19] L. Kotchenda,[25] V. Kouchpil,[10] K.L. Kowalik,[21] M. Kramer,[26] P. Kravtsov,[25] V.I. Kravtsov,[31] K. Krueger,[1] C. Kuhn,[17] A.I. Kulikov,[11] A. Kumar,[29] A.A. Kuznetsov,[11] M.A.C. Lamont,[49] J.M. Landgraf,[3] S. Lange,[13] S. LaPointe,[47] F. Laue,[3] J. Lauret,[3] A. Lebedev,[3] R. Lednicky,[12] C-H. Lee,[33] S. Lehocka,[11] M.J. LeVine,[3] C. Li,[37] Q. Li,[47] Y. Li,[42] G. Lin,[49] S.J. Lindenbaum,[26] M.A. Lisa,[28] F. Liu,[48] H. Liu,[37] J. Liu,[35] L. Liu,[48] Z. Liu,[48] T. Ljubicic,[3] W.J. Llope,[35] H. Long,[7] R.S. Longacre,[3] M. Lopez-Noriega,[28] W.A. Love,[3] Y. Lu,[48] T. Ludlam,[3] D. Lynn,[3] G.L. Ma,[38] J.G. Ma,[7] Y.G. Ma,[38] D. Magestro,[28] D.P. Mahapatra,[14] R. Majka,[49] L.K. Mangotra,[18] R. Manweiler,[43] S. Margetis,[19] C. Markert,[19] L. Martin,[39] H.S. Matis,[21] Yu.A. Matulenko,[31] C.J. McClain,[1] T.S. McShane,[9] Yu. Melnick,[31] A. Meschanin,[31] M.L. Miller,[22] N.G. Minaev,[31] S. Mioduszewski,[40] C. Mironov,[19] A. Mischke,[27] D.K. Mishra,[14] J. Mitchell,[35] B. Mohanty,[44] L. Molnar,[32] C.F. Moore,[41] D.A. Morozov,[31] M.G. Munhoz,[36] B.K. Nandi,[15] C. Nattrass,[49] T.K. Nayak,[44] J.M. Nelson,[2] P.K. Netrakanti,[44] V.A. Nikitin,[12] L.V. Nogach,[31] S.B. Nurushev,[31] G. Odyniec,[21] A. Ogawa,[3] V. Okorokov,[25] M. Oldenburg,[21] D. Olson,[21] M. Pachr,[10] S.K. Pal,[44] Y. Panebratsev,[11] S.Y. Panitkin,[3] A.I. Pavlinov,[47] T. Pawlak,[45] T. Peitzmann,[27] V. Perevoztchikov,[3] C. Perkins,[5] W. Peryt,[45] V.A. Petrov,[47] S.C. Phatak,[14] R. Picha,[6] M. Planinic,[50] J. Pluta,[45] N. Poljak,[50] N. Porile,[32] J. Porter,[46] A.M. Poskanzer,[21] M. Potekhin,[3] E. Potrebenikova,[11] B.V.K.S. Potukuchi,[18] D. Prindle,[46] C. Pruneau,[47] J. Putschke,[21] G. Rakness,[30] R. Raniwala,[34] S. Raniwala,[34] R.L. Ray,[41] S.V. Razin,[11] J. Reinnarth,[39] D. Relyea,[4] F. Retiere,[21] A. Ridiger,[25] H.G. Ritter,[21] J.B. Roberts,[35] O.V. Rogachevskiy,[11] J.L. Romero,[6] A. Rose,[21] C. Roy,[39] L. Ruan,[21] M.J. Russcher,[27] R. Sahoo,[14] I. Sakrejda,[21] S. Salur,[49] J. Sandweiss,[49] M. Sarsour,[40] P.S. Sazhin,[11] J. Schambach,[41] R.P. Scharenberg,[32] N. Schmitz,[23] K. Schweda,[21] J. Seger,[9] I. Selyuzhenkov,[47] P. Seyboth,[23] A. Shabetai,[21] E. Shahaliev,[11] M. Shao,[37] M. Sharma,[29] W.Q. Shen,[38] S.S. Shimanskiy,[11] E Sichtermann,[21] F. Simon,[22] R.N. Singaraju,[44] N. Smirnov,[49] R. Snellings,[27] G. Sood,[43] P. Sorensen,[3] J. Sowinski,[16] J. Speltz,[17] H.M. Spinka,[1] B. Srivastava,[32] A. Stadnik,[11] T.D.S. Stanislaus,[43] R. Stock,[13] A. Stolpovsky,[47] M. Strikhanov,[25] B. Stringfellow,[32] A.A.P. Suaide,[36] E. Sugarbaker,[28] M. Sumbera,[10] Z. Sun,[20] B. Surrow,[22] M. Swanger,[9] T.J.M. Symons,[21] A. Szanto de Toledo,[36] A. Tai,[7] J. Takahashi,[36] A.H. Tang,[3] T. Tarnowsky,[32] D. Thein,[7] J.H. Thomas,[21] A.R. Timmins,[2] S. Timoshenko,[25] M. Tokarev,[11] T.A. Trainor,[46] S. Trentalange,[7] R.E. Tribble,[40] O.D. Tsai,[7] J. Ulery,[32] T. Ullrich,[3] D.G. Underwood,[1] G. Van Buren,[3] N. van der Kolk,[27] M. van Leeuwen,[21] A.M. Vander Molen,[24] R. Varma,[15] I.M. Vasilevski,[12] A.N. Vasiliev,[31] R. Vernet,[17] S.E. Vigdor,[16] Y.P. Viyogi,[44] S. Vokal,[11] S.A. Voloshin,[47] W.T. Waggoner,[9] F. Wang,[32] G. Wang,[19] J.S. Wang,[20] X.L. Wang,[37] Y. Wang,[42] J.W. Watson,[19] J.C. Webb,[16] G.D. Westfall,[24] A. Wetzler,[21] C. Whitten Jr.,[7] H. Wieman,[21] S.W. Wissink,[16] R. Witt,[49] J. Wood,[7] J. Wu,[37] N. Xu,[21] Q.H. Xu,[21] Z. Xu,[3] P. Yepes,[35] I-K. Yoo,[33] V.I. Yurevich,[11] W. Zhan,[20] H. Zhang,[3] W.M. Zhang,[19] Y. Zhang,[37]

Z.P. Zhang,[37] Y. Zhao,[37] C. Zhong,[38] R. Zoulkarneev,[12] Y. Zoulkarneeva,[12] A.N. Zubarev,[11] and J.X. Zuo[38]
(STAR Collaboration)

[1] *Argonne National Laboratory, Argonne, Illinois 60439*
[2] *University of Birmingham, Birmingham, United Kingdom*
[3] *Brookhaven National Laboratory, Upton, New York 11973*
[4] *California Institute of Technology, Pasadena, California 91125*
[5] *University of California, Berkeley, California 94720*
[6] *University of California, Davis, California 95616*
[7] *University of California, Los Angeles, California 90095*
[8] *Carnegie Mellon University, Pittsburgh, Pennsylvania 15213*
[9] *Creighton University, Omaha, Nebraska 68178*
[10] *Nuclear Physics Institute AS CR, 250 68 Řež/Prague, Czech Republic*
[11] *Laboratory for High Energy (JINR), Dubna, Russia*
[12] *Particle Physics Laboratory (JINR), Dubna, Russia*
[13] *University of Frankfurt, Frankfurt, Germany*
[14] *Institute of Physics, Bhubaneswar 751005, India*
[15] *Indian Institute of Technology, Mumbai, India*
[16] *Indiana University, Bloomington, Indiana 47408*
[17] *Institut de Recherches Subatomiques, Strasbourg, France*
[18] *University of Jammu, Jammu 180001, India*
[19] *Kent State University, Kent, Ohio 44242*
[20] *Institute of Modern Physics, Lanzhou, China*
[21] *Lawrence Berkeley National Laboratory, Berkeley, California 94720*
[22] *Massachusetts Institute of Technology, Cambridge, MA 02139-4307*
[23] *Max-Planck-Institut für Physik, Munich, Germany*
[24] *Michigan State University, East Lansing, Michigan 48824*
[25] *Moscow Engineering Physics Institute, Moscow Russia*
[26] *City College of New York, New York City, New York 10031*
[27] *NIKHEF and Utrecht University, Amsterdam, The Netherlands*
[28] *Ohio State University, Columbus, Ohio 43210*
[29] *Panjab University, Chandigarh 160014, India*
[30] *Pennsylvania State University, University Park, Pennsylvania 16802*
[31] *Institute of High Energy Physics, Protvino, Russia*
[32] *Purdue University, West Lafayette, Indiana 47907*
[33] *Pusan National University, Pusan, Republic of Korea*
[34] *University of Rajasthan, Jaipur 302004, India*
[35] *Rice University, Houston, Texas 77251*
[36] *Universidade de Sao Paulo, Sao Paulo, Brazil*
[37] *University of Science & Technology of China, Hefei 230026, China*
[38] *Shanghai Institute of Applied Physics, Shanghai 201800, China*
[39] *SUBATECH, Nantes, France*
[40] *Texas A&M University, College Station, Texas 77843*
[41] *University of Texas, Austin, Texas 78712*
[42] *Tsinghua University, Beijing 100084, China*
[43] *Valparaiso University, Valparaiso, Indiana 46383*
[44] *Variable Energy Cyclotron Centre, Kolkata 700064, India*
[45] *Warsaw University of Technology, Warsaw, Poland*
[46] *University of Washington, Seattle, Washington 98195*
[47] *Wayne State University, Detroit, Michigan 48201*
[48] *Institute of Particle Physics, CCNU (HZNU), Wuhan 430079, China*
[49] *Yale University, New Haven, Connecticut 06520*
[50] *University of Zagreb, Zagreb, HR-10002, Croatia*

(Dated: February 8, 2008)

We present the scaling properties of Λ, Ξ, Ω and their anti-particles produced at mid-rapidity in $Au+Au$ collisions at RHIC at $\sqrt{s_{NN}} = 200$ GeV. The yield of multi-strange baryons per participant nucleon increases from peripheral to central collisions more rapidly than the Λ yield, which appears to correspond to an increasing strange quark density of matter produced. The value of the strange phase space occupancy factor γ_s, obtained from a thermal model fit to the data, approaches unity for the most central collisions. We also show that the nuclear modification factors, R_{CP}, of Λ and Ξ are consistent with each other and with that of protons in the transverse momentum range 2.0 $< p_T <$ 5.0 GeV/c. This scaling behaviour is consistent with a scenario of hadron formation from constituent quark degrees of freedom through quark recombination or coalescence.

PACS numbers: 25.75.Dw

Lattice Quantum ChromoDynamics calculations predict that a new state of matter, the Quark Gluon Plasma (QGP), can be formed at zero baryon density in nuclear collisions when the temperature exceeds $160 - 170$ MeV [1]. Strange quarks, whose mass is comparable to the critical temperature, are expected to be abundantly produced by thermal parton interactions in the high temperature QGP phase. Due to the corresponding increase in the strange quark density, hyperon production is expected to be enhanced in high energy nuclear collisions, the enhancement increasing with the number of strange valence quarks in the hyperon [2]. Such an effect has already been observed in various fixed-target experiments at lower energy by comparing the number of hyperons produced per participating nucleon in nucleus-nucleus and proton-nucleus collisions [3, 4, 5]. In this letter, we study the centrality dependence of hyperon production in $Au + Au$ collisions at a collision energy of $\sqrt{s_{NN}} = 200$ GeV, which is an order of magnitude higher than that previously achieved. We also study the transverse momentum dependence of hyperon production in central and peripheral collisions in an attempt to shed light upon the possible production mechanisms.

Previous studies have shown that ratios of hadron yields in high energy nucleus-nucleus collisions are generally well described by statistical models in the grand canonical limit, where baryo-chemical potential and temperature are parameters [6, 7, 8]. A strangeness phase-space occupancy factor, γ_s, is sometimes introduced to describe the extent to which strangeness reaches its equilibrium abundance. In this framework, the amount of strangeness produced per participating nucleon (N_{part}) is directly related to the value of γ_s. The centrality dependence of γ_s therefore provides a quantitative measure of strangeness equilibration as a function of system size in nucleus-nucleus collisions [9], under the assumption that the grand canonical approximation remains valid in non-central collisions.

By contrast, at high transverse momentum, hadrons are thought to be produced via incoherent hard scatterings, which, in the absence of any nuclear medium effects, should scale with the number of binary nucleon-nucleon collisions (N_{binary}) [10, 11]. Measurements of hadron production in $Au + Au$ collisions at RHIC have shown that not only is there a deviation from binary scaling in central collisions [10, 12], but also a distinct difference in the scaling behaviour of baryons and mesons in the intermediate transverse momentum range, $2 < p_T < 5$ GeV/c [13, 14]. A strong particle-type dependence is not predicted by conventional Monte Carlo (MC) event simulators such as HIJING, where hadron formation in this region is dominated by independent parton fragmentation [15]. On the other hand, quark recombination (coalescence) models have been successful in explaining the observed deviation from binary scaling for baryons and mesons in central collisions [16, 17, 18, 19], as well as providing an explanation for the particle-type dependence of measured azimuthal anisotropies at intermediate p_T in non-central collisions [14]. By extending these previous studies to include multi-strange baryons we provide a more stringent test of recombination models. Furthermore, it may allow us to probe the differences between strange and light (up and down) quark distributions produced in nucleus-nucleus collisions.

The STAR Time Projection Chamber (TPC) measures the trajectories and momenta of charged particles produced in each collision in the pseudo-rapidity range $|\eta| < 1.8$ [20]. The detector operates within a solenoidal magnetic field of 0.5 Tesla whose axis is aligned with the beam. A central trigger barrel, covering the pseudo-rapidity region $|\eta| < 1$, and two zero-degree calorimeters are used as trigger detectors. A total of 1.6×10^6 minimum-bias trigger collisions and 1.5×10^6 central trigger collisions were used for this analysis. A detailed description of the analysis including particle reconstruction, track quality, decay vertex topology cuts and calculation of the detection efficiency can be found elsewhere [21, 22, 23]. In this study $\Lambda(\overline{\Lambda})$, $\Xi^-(\overline{\Xi}^+)$ and $\Omega^-(\overline{\Omega}^+)$ have been measured in rapidity intervals of $|y| < 1$, 0.75 and 0.75, respectively. In order to increase statistics, the results for Ω^- and $\overline{\Omega}^+$ have been combined. Within the chosen rapidity intervals the particle reconstruction efficiency is a function of transverse momentum and lifetime. The efficiency calculations were based on the probability of finding Monte Carlo generated particles after processing them through a TPC detector response simulation, embedding them into real events and then reconstructing them as real data. The collision centrality was defined by the charged particle multiplicity measured in the TPC in the pseudo-rapidity range $|\eta| < 0.5$. Five centrality bins were selected corresponding to the following ranges in the total hadronic cross section ($0 - 5\%$, $10 - 20\%$, $20 - 40\%$, $40 - 60\%$, $60 - 80\%$). The $0 - 5\%$ bin represents the most central collisions and was obtained from the central trigger sample. The remaining bins were obtained from the minimum-bias sample. Due to relatively poor statistics, the 5-10% bin and the Ω 10-20% and 60-80% bins were omitted from this analysis.

Figure 1 shows the transverse momentum distributions of $\Lambda(\overline{\Lambda})$, $\Xi^-(\overline{\Xi}^+)$ and $\Omega^- + \overline{\Omega}^+$ measured at mid-rapidity and as function of centrality. The errors shown on the data points are statistical only. The Λ spectra were corrected for feed-down from multi-strange baryon weak decays, based upon the measured Ξ and Ω spectra. The feed-down correction depends sensitively on both exper-

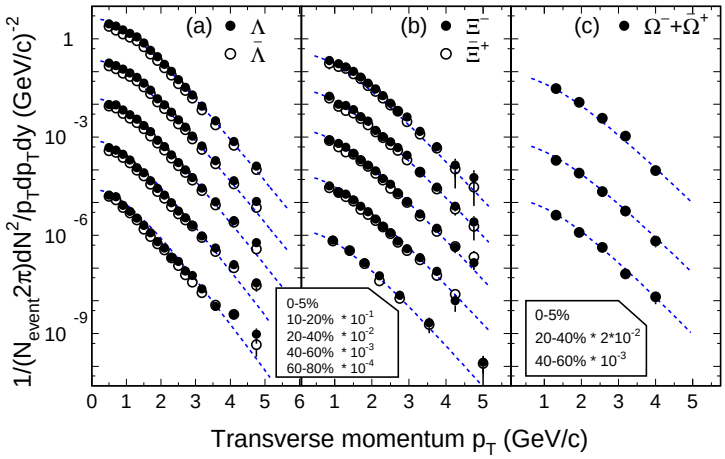

FIG. 1: Transverse momentum distributions of (a) $\Lambda(\overline{\Lambda})$ for $|y| < 1.0$, (b) Ξ^- ($\overline{\Xi}^+$) for $|y| < 0.75$ and (c) $\Omega^- + \overline{\Omega}^+$ for $|y| < 0.75$ in $Au + Au$ collisions at $\sqrt{s_{NN}} = 200$ GeV as a function of centrality. The Λ spectra were corrected for weak decay of Ξ, Ξ^0 and Ω. Scale factors were applied to the spectra for clarity. Only statistical errors are shown. The dashed curves show a Boltzmann fit to the Λ, Ξ^- and $\Omega^- + \overline{\Omega}^+$ data, the fits to the $\overline{\Lambda}$ and $\overline{\Xi}^+$ are omitted for clarity.

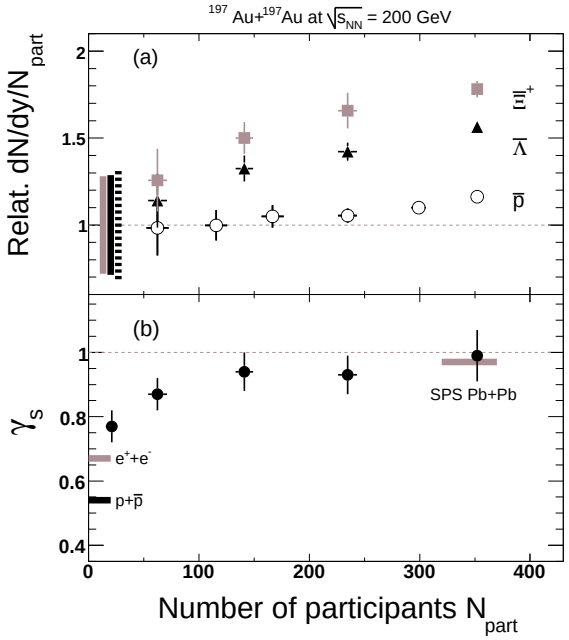

FIG. 2: (a) The corrected integrated yield dN/dy at mid-rapidity for $\overline{\Xi}^+$, $\overline{\Lambda}$ and $\bar{p}$ divided by N_{part}, normalized to the most peripheral centrality interval $(60-80\%)$, plotted as a function of N_{part}. The gray, black and dashed bands represent the errors on the normalization to the most peripheral bin for the $\bar{\Xi}^+$, $\bar{\Lambda}$ and $\bar{p}$. Other errors shown are statistical only. (b) γ_s as a function of N_{part} calculated from thermal model fits to the measured particle yields (π,K,p [24], Λ, Ξ, Ω and their anti-particles) at 200 GeV. Values for $e^+ + e^-$ and p+$\bar{\text{p}}$ collisions at $\sqrt{s_{NN}} = 91$ and 200 GeV respectively and for Pb+Pb SPS collisions at $\sqrt{s_{NN}} = 17.2$ GeV are shown for comparison [26, 27, 28].

imental acceptance and the cuts used in the analysis. The contribution to the Λ spectrum from Ξ and Ω decays is at the 15% level. The feed-down contribution to the Ξ spectrum from Ω decays is negligible. The measured p_T coverage is about 70% for Λ and 60% for Ξ and Ω. The total integrated yields (dN/dy) were extracted from Boltzmann fits to the spectra and are presented in Table I.

The systematic error on the reconstructed yields was studied as a function of p_T. Three main factors contribute to the systematic error: (i) subtle differences between the Monte Carlo simulation and real data, which make the reconstructed yields sensitive to the choice of geometric cuts used to improve the signal to background ratio, (ii) sensitivity to the method used to subtract the remaining background after geometric cuts have been applied, and (iii) measured differences in the yield dependent on the direction of the applied magnetic field. At low p_T, the dominant contribution to the systematic error is due to the choice of cuts. Here, the systematic error was estimated by varying the cuts about their optimal values and observing the change in the reconstructed yield. At high p_T the systematic error is dominated by the differences observed in the reconstructed yield for the two magnetic field settings. In order to determine the systematic uncertainty on the total yield and the inverse slope parameter for each particle and centrality class, p_T dependent systematic errors were added to the data points shown in figure 1 and included in a second fit. The systematic errors shown in Table I reflect the difference between the two fits. We also investigated the choice of function used to fit the data. Although the Boltzmann function gave a better fit, an exponential function could not be excluded. Exponential fits to the data gave a 5-6% higher yield on average and a larger inverse slope parameter by 40-50 MeV. These differences are not included in the errors shown in Table I.

Figure 2(a) presents the strange anti-particle yields, dN/dy, divided by N_{part}. For clarity, only statistical errors are shown. All data points are normalized to the values obtained in the most peripheral collisions (centrality bin $60-80\%$). The centrality dependence of the anti-proton yield is also shown for comparison [24]. Strange anti-particles are chosen because all valence quarks must have been created in the collision, although similar results are also obtained for strange particles. In a geometrical description of nuclear collisions the number of participant nucleons is proportional to the initial overlapping volume of the colliding nuclei. The integrated yield is dominated by the low p_T region where particle production originates from mainly soft (non-perturbative) processes. The integrated yield per participating nucleon may be a measure of the formation probability of a hadron from the bulk. As such, we would expect it to be sensitive to the density of the hadron's constituent quarks in the system. We note that there appears to be a

Centrality	0–5%	10–20%	20–40%	40–60%	60–80%
$< N_{part} >$	352±3	235±9	141±8	62±9	21±6
Λ	16.7±0.2±1.1	10.0±0.1±0.7	5.53±0.05±0.39	2.07±0.03±0.14	0.58±0.01±0.04
	309±1±8	308±1±8	303±1±8	297±2±10	287±3±10
$\overline{\Lambda}$	12.7±0.2±0.9	7.7±0.1±0.5	4.30±0.04±0.30	1.64±0.03±0.11	0.48±0.01±0.03
	310±1±7	309±1±8	306±1±9	298±2±10	282±3±10
Ξ^-	2.17±0.06±0.19	1.41±0.04±0.08	0.72±0.02±0.02	0.26±0.01±0.02	0.063±0.004±0.003
	335±4±7	331±4±8	326±3±6	325±4±7	320±8±13
$\overline{\Xi}^+$	1.83±0.05±0.20	1.14±0.04±0.08	0.62±0.02±0.03	0.23±0.01±0.02	0.061±0.004±0.002
	335±4±9	334±4±9	327±3±6	327±5±7	302±8±16
$\Omega + \overline{\Omega}^+$	0.53±0.04±0.04	-	0.17±0.02±0.01	0.063±0.008±0.004	-
	353±9±10	-	348±15±12	336±17±13	-

TABLE I: Integrated yields dN/dy and inverse slope parameters T (MeV) extracted from a Boltzmann fit to the p_T spectra of $\Lambda(\overline{\Lambda})$, $\Xi^-(\overline{\Xi})^+$ and $\Omega^- + \overline{\Omega}^+$ at mid-rapidity. Statistical and systematic errors are presented. Also shown for each centrality is $< N_{part} >$, the number of participants, extracted from a Monte Carlo Glauber model calculation [10, 11].

hierachy of particle production dependent upon strange-quark content, which has also been observed at lower energies [3, 5]. This may reflect an increase in the strange quark density in more central collisions.

Thermal-statistical models have been very successful in describing particle yields in various systems at different energies [6, 7]. Within such models, the densities of strange particles, including strange resonances, are governed by statistical laws. The possible non-equilibrium of strange quarks is taken into account by introducing a phase space occupancy factor, γ_s. With the measured yields of strange baryons and other hadrons, such as pions, kaons, protons and their anti-particles [24], we have performed a fit using the statistical model described in [25] to determine γ_s as a function of the number of participants, as shown in figure 2(b). We find that the value of γ_s increases from about 0.8 in peripheral collisions to about 1.0 in central collisions. In each case we obtained a freeze-out temperature around 165 MeV. According to the model, the Λ yield depends linearly on γ_s while the yield of Ξ depends on γ_s^2. This is consistent with behavior observed in figure 2(a). The fact that γ_s approaches unity when $N_{part} > 150$ suggests that the strange quark abundance tends to equilibrate as the system-size increases. A recent analysis of hadron yields in nucleus-nucleus collisions at $\sqrt{s_{NN}} = 17.2$ GeV, using a different thermal model, also found that γ_s approaches unity at mid-rapidity in central collisions [26], whereas statistical analyses of elementary e^++e^- and p+$\bar{p}$ collisions at various energies yield a value of γ_s significantly less than unity [27, 28].

We studied the effect of including different combinations of particles in the fit and found that particle ratios involving protons and Λ are important in constraining the freeze-out temperature and γ_s, respectively. The value and centrality dependence of γ_s is relatively insensitive to the inclusion of other particle ratios in the fit. The errors shown in figure 2(b) reflect the variation of γ_s found in this study.

In order to investigate the scaling behaviour of hyperon production in the intermediate transverse momentum region, figure 3 shows the nuclear modification factor (R_{CP}) [14] for $\Xi^- + \overline{\Xi}^+$ and $\Omega + \overline{\Omega}$. The nuclear modification factor was found by forming the ratio of the p_T spectra of the $0-5\%$ and $40-60\%$ centrality bins, after normalising each spectrum to the average number of binary collisions, appropriate for each centrality range, obtained from a Monte Carlo Glauber calculation [10, 11]. The $40-60\%$ centrality bin was chosen as the reference because of the limited statistics of $\Omega + \overline{\Omega}$ in the

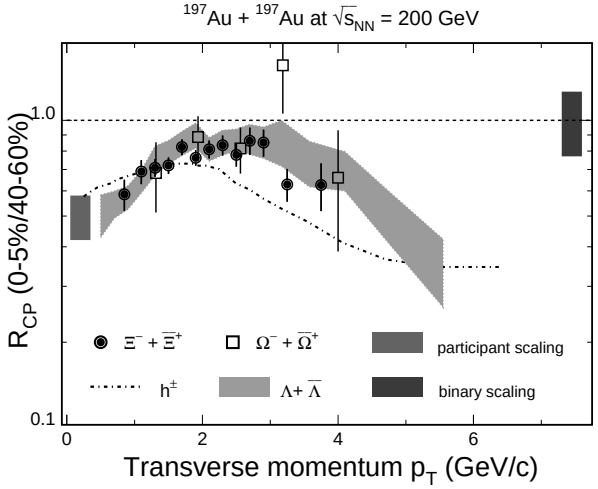

FIG. 3: R_{CP} for $\Xi^- + \overline{\Xi}^+$ and $\Omega^- + \overline{\Omega}^+$ at mid-rapidity (centrality interval : $0-5\%$ vs. $40-60\%$). A dashed line for charged hadrons and gray band for $\Lambda + \overline{\Lambda}$ are shown as comparison. The gray rectangles represent participant and binary scalings.

$60-80\%$ bin. Also shown in figure 3 are the previously published results for charged hadrons and $\Lambda+\overline{\Lambda}$ for the same centrality bins [14]. The dark gray rectangular boxes on the plot represent the expected R_{CP} range for N_{part} and N_{bin} scalings, indicating the range of uncertainty in calculating the number of participants and of binary collisions for each centrality. Although the p_T integrated yield per participating nucleon of Ξ increases faster with N_{part} than for Λ hyperons, in the interval $1.8 < p_T < 3.5$ GeV/c, the p_T dependence of R_{CP} for $\Xi^- + \overline{\Xi}^+$ and $\Omega^- + \overline{\Omega}^+$ are similar and coincide with the trend previously shown for $\Lambda+\overline{\Lambda}$. The R_{CP} of hyperons exhibits little suppression while mesons (approximated by the dashed line) have a distinctly different trend. The difference in R_{CP} for baryons and mesons in the intermediate p_T region has previously been discussed in the framework of recombination (or coalescence) models [12, 14, 16, 29]. The results presented here appear to confirm that the difference is dependent upon the number of constituent quarks and is not a mass effect. Further weight is given to this argument by a recent measurement of the nuclear modification factor of protons [13], $K(892)^*$ [30] and ϕ mesons [31]. The similarity between Λ and Ξ R_{CP} at intermediate p_T reinforces the notion of a baryon-meson difference. Futhermore, it suggests that the strange quark distribution scales with centrality in a similar way to up and down quarks, since baryons with different strangeness content seem to follow the same pattern. This observation is consistent with recent elliptic flow measurements of Λ, Ξ and Ω at intermediate p_T [32].

In this letter, we have presented the scaling properties of strange baryon production in $Au+Au$ collisions at $\sqrt{s_{NN}} = 200$ GeV. By studying the hyperon yields scaled by N_{part} and the centrality dependence of γ_s within the framework of a thermal model, we have found that strangeness equilibrium appears to have been achieved in central collisions at RHIC. We have also investigated the centrality dependence of the transverse momentum distributions of hyperons. We find that hyperon yields in central collisions fall below the expectation for binary scaling for $p_T > 3$ GeV/c and that the nuclear modification factor R_{CP} is similar for all hyperons independent of their mass or strangeness content. In addition we note that the R_{CP} of hyperons is similar to that of protons, a feature that is consistent with models of hadron formation based upon quark recombination.

Acknowledgments: We thank the RHIC Operations Group and RCF at BNL, and the NERSC Center at LBNL for their support. This work was supported in part by the HENP Divisions of the Office of Science of the U.S. DOE; the U.S. NSF; the BMBF of Germany; IN2P3, RA, RPL, and EMN of France; EPSRC of the United Kingdom; FAPESP of Brazil; the Russian Ministry of Science and Technology; the Ministry of Education and the NNSFC of China; SFOM of the Czech Republic, FOM and UU of the Netherlands, DAE, DST, and CSIR of the Government of India; the Swiss NSF.

[1] Z. Fodor and S.D. Katz, JHEP 04:050 (2004).
[2] J. Rafelski and B. Muller, Phys. Rev. Lett. **48**, 1066 (1982).
[3] E. Andersen *et al.*, WA97 Collaboration, Phys. Lett. **B 449**, 401 (1999).
[4] S. V. Afanasiev *et al.*, NA49 Collaboration, Nucl. Phys. **A 698**, 104 (2002).
[5] F. Antinori *et al.*, WA97/NA57 Collaboration, Nucl. Phys. **A 698**, 118 (2002).
[6] P. Braun-Munzinger *et al.*, Phys. Lett. **B 518**, 41(2001).
[7] J. Rafelski and J. Letessier, Nucl. Phys. **A 715**, 98 (2003).
[8] F. Becattini and L. Ferroni, Eur. Phys. J. **C 38**, 225 (2004).
[9] J. Cleymans, B. Kaempfer, P. Steinberg and S. Wheaton, J. Phys.**G 30**, S595 (2004)
[10] C. Adler *et al.*, STAR Collaboration, Phys. Rev. Lett. **89**, 202301 (2002).
[11] R. J. Glauber, Lectures on Theoretical Physics, Vol. 1, 315 (1959).
[12] K. Adcox *et al.*, PHENIX Collaboration, Phys. Rev. Lett. **88**, 022301 (2002).
[13] S. S. Adler *et al.*, PHENIX Collaboration, Phys. Rev. **C 69**, 034909 (2004).
[14] J. Adams *et al.*, STAR Collaboration, Phys. Rev. Lett. **92**, 052302 (2004).
[15] B. Andersson *et al.*, Phys. Rept. **97**, 31 (1983); B. Andersson, G. Gustafson and B. Soderberg, Z. Phys. **C 20**, 317 (1983); X. Artru and G. Mennessier, Nucl. Phys. **B70**, 93 (1974); X. Artru, Phys. Rept. **97**, 147 (1983).
[16] R. J. Fries *et al.*, Phys. Rev. **C 68**, 044902 (2003).
[17] D. Molnar and S. A. Voloshin, Phys. Rev. Lett. **91**, 092301 (2003).
[18] V. Greco, C. M. Ko and P. Levai, Phys. Rev. **C 68**, 034904 (2003).
[19] Z. W. Lin and C. M. Ko, Phys. Rev. Lett. **89**, 202302 (2002).
[20] M. Anderson *et al.*, STAR Collaboration, Nucl. Instrum. Meth. **A 499**, 659 (2003)
[21] K. H. Ackermann *et al.*, STAR Collaboration, Phys. Rev. Lett. **86**, 402 (2001).
[22] C. Adler *et al.*, STAR Collaboration, Phys. Rev. Lett. **89**, 092301 (2002).
[23] J. Adams *et al.*, STAR Collaboration, Phys. Rev. Lett. **92**, 182301 (2004).
[24] J. Adams *et al.*, STAR Collaboration, Phys. Rev. Lett. **92**, 112301 (2004).
[25] J. Cleymans *et al.*, Phys. Rev. **C 71**, 054901 (2005).
[26] F. Becattini *et al.*, Phys. Rev. **C 69**, 024905 (2004).
[27] F. Becattini, Z. Phys. **C 69**, 485 (1996).
[28] F. Becattini and U. Heinz, Z. Phys. **C 76**, 269 (1997).
[29] R. C. Hwa and C. B. Yang, Phys. Rev. **C 67**, 034902 (2003).
[30] J. Adams *et al.*, STAR Collaboration, Phys. Rev. **C 71**, 064902 (2005).
[31] J. Adams *et al.*, STAR Collaboration, Phys. Lett. **B 612**, 181 (2005).

[32] J. Adams *et al.*, STAR Collaboration, Phys. Rev. Lett. **95**, 122301 (2005).

This work was supported by the U.S. Department of Energy under Contract Number DE-AC02-05CH11231.